

## Paramagnetic resonance of $Gd^{3+}$ as a probe of exchange and crystal-field effects in singlet-ground-state systems\*

K. Sugawara and C. Y. Huang

*Department of Physics, Case Western Reserve University,<sup>†</sup> Cleveland, Ohio 44106*

Bernard R. Cooper

*Department of Physics, West Virginia University, Morgantown, West Virginia 26506*

(Received 26 December 1974)

We have studied the use of paramagnetic resonance of dilute Gd impurities as a probe of exchange and crystal-field effects in the singlet-ground-state systems  $TmX$  and  $PrX$  (where  $X$  is one of the group-VA elements, P, As, Sb, Bi), i.e., the thulium and praseodymium monopnictides of NaCl structure. Analysis of the temperature-dependent resonance  $g$ -value behavior yields values for the Gd-Tm and Gd-Pr exchange interactions. The Gd-Tm exchange changes sign with increasing lattice parameter (on going from the phosphide and arsenide to the antimonide and bismuthide); while the Gd-Pr exchange becomes increasingly negative with increasing lattice parameter. Analysis of the temperature dependence of the linewidth yields values for the crystal-field splitting of  $Tm^{3+}$  and  $Pr^{3+}$  in agreement with those from neutron scattering. We briefly mention recent experiments using EPR of Gd in TbP to probe the behavior of the staggered susceptibility in the critical region.

### I. INTRODUCTION

There has been much interest in recent years in the magnetic properties of rare-earth systems where the rare earth has a crystal-field-only singlet ground state.<sup>1,2</sup> The occurrence of magnetic ordering in such systems depends on a competition between exchange and crystal-field effects.<sup>1</sup> While the dominance of crystal-field effects explains the lack of magnetic ordering in compounds such as the thulium and praseodymium monopnictides and this dominance also explains the basic features of susceptibility and high-field magnetization measurements, understanding of the magnetic behavior is not complete, particularly with regard to the role played by exchange in dynamic effects. We have used two types of paramagnetic resonance experiments to study paramagnetic singlet-ground-state systems. In one type of experiment, as recently reported,<sup>3(a)</sup> we study the paramagnetic resonance in one of the crystal-field excited states of the rare earth in a pure concentrated paramagnetic singlet-ground-state system. In the second type of experiment, as reported here, we study the paramagnetic resonance of dilute Gd impurities used as a probe of the magnetic behavior of such a system.<sup>3(b)</sup> These studies provide information on the exchange and crystal-field effects in the singlet-ground-state systems of interest. Obtaining this information depends on the fact that the resonance  $g$  values and line widths of the Gd impurities serve to probe the behavior of the isothermal and isolated susceptibilities of the host materials. (The isothermal susceptibility is the susceptibility measured under circumstances where the spin system remains in thermal equilibrium with the lattice during the

measurement period. This means that the thermal populations of the various crystal-field levels adjust themselves in a way corresponding to the change in Boltzmann factors as the energies of the levels change with magnetic field. The isolated susceptibility is that measured when the thermal populations of the levels do not change. The effect measured is due to the change in wave functions, and hence moments, with field, i.e., the polarization effect.)

As shown in Fig. 1, the ground state of both  $Tm^{3+}$  and  $Pr^{3+}$  with fourth-order crystal-field anisotropy

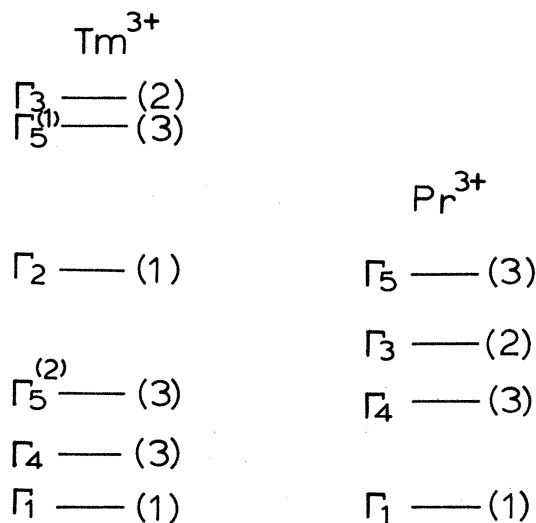


FIG. 1. Crystal-field energy levels for  $Tm^{3+}$  and  $Pr^{3+}$  in octahedral environment when fourth-order crystal-field anisotropy is dominant.

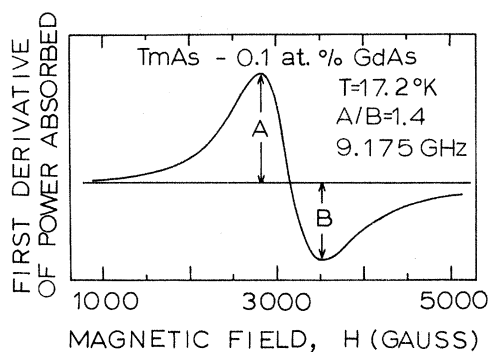


FIG. 2. Shape of the EPR absorption of  $Gd^{3+}$  for TmAs-0.1-at. % GdAs at 9.1 GHz.

dominant in the NaCl-structure monpnictides is a singlet  $\Gamma_1$  state; and the order of magnitude of the energy separation between the ground state and the first excited state is between 10 and 100 °K. Therefore one expects that the most interesting behavior of the EPR of the Gd impurities would occur in the temperature range between 4.2 and 300 °K. We have studied the EPR of  $Gd^{3+}$  with nominal concentration between 0.05 and 10 at. % in PrP, PrAs, PrSb, and PrBi and with nominal concentration between 0.1 and 10 at. % in TmP, TmAs, TmSb, and TmBi. We have used our results for temperature dependence of the  $Gd^{3+}$  EPR  $g$  shift and linewidth to obtain values for the Gd-Pr and Gd-Tm exchange interaction and for the crystal-field splitting in the host monopnictide.

## II. SAMPLE PREPARATION AND EPR SPECTROMETER

A number of samples of  $n$ -at. % GdX in TmX and  $n$ -at. % GdX in PrX ( $n$  is less than 10,  $X=P, As, Sb, Bi$ ) were prepared in powdered form. The alloys  $Gd_xR_{1-x}$ , where  $R$  is Pr or Tm, were first made by using an electric induction heater. The two constituents, Gd and  $R$ , were heated in a tantalum crucible under argon atmosphere for about

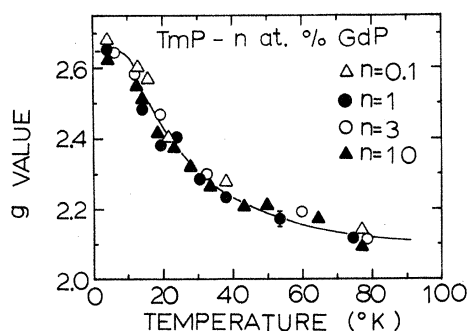


FIG. 3. Temperature dependence of EPR  $g$  value of  $Gd^{3+}$  in TmP- $n$ -at. % GdP ( $n=0.1, 1, 3, 10$ ).

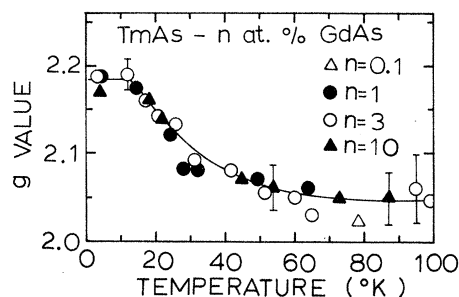


FIG. 4. Temperature dependence of EPR  $g$  value of  $Gd^{3+}$  in TmAs- $n$ -at. % GdAs ( $n=0.1, 1, 3, 10$ ).

1 h for  $Gd_xPr_{1-x}$  and for about 20 or 30 min for  $Gd_xTm_{1-x}$ . For  $Gd_xTm_{1-x}$ , because of the high vapor pressure of Tm metal, it was necessary to use an argon pressure of 2 or 3 atm. After making the alloys in this manner, turnings of the alloys were prepared. Thereafter the process for making the intermetallic compounds with the group-V A elements is as given by Jones.<sup>4</sup> The purities of the rare-earth metals and group-V A elements used were higher than 99.9% and 99.999%, respectively. Standard x-ray powder diffraction techniques were used to confirm that the samples had the correct rock-salt structure and lattice constants.

Our EPR spectrometer is a conventional one operating at 9.1 GHz.

## III. REVIEW OF THE THEORY $g$ SHIFT DUE TO Gd-HOST EXCHANGE AND OF THEORY OF THE RESONANCE LINE WIDTH

Our major interest is to study the exchange interaction between  $Gd^{3+}$  ion and the surrounding host rare-earth ions and to study the crystal-field splitting of the host rare-earth ions. The isothermal susceptibility of the host rare-earth ion affects the  $g$  value of  $Gd^{3+}$  via the exchange interaction between them; and the spin fluctuations of the host ion determine the linewidth of  $Gd^{3+}$ . In

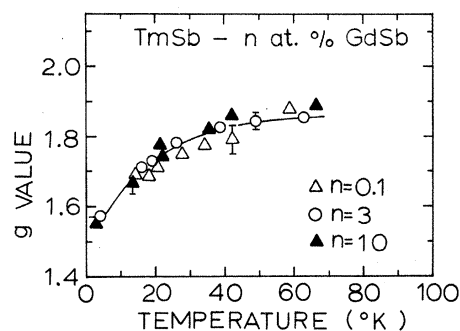


FIG. 5. Temperature dependence of EPR  $g$  value of  $Gd^{3+}$  in TmSb- $n$ -at. % GdSb ( $n=0.1, 3, 10$ ).

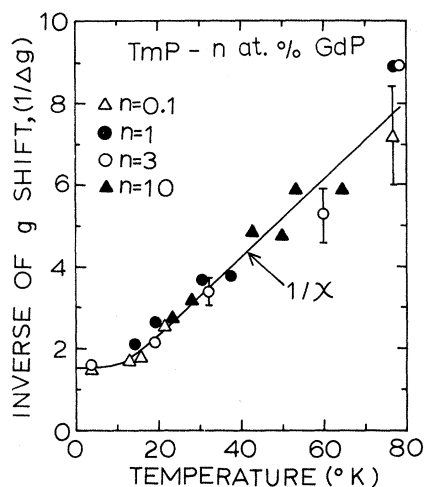


FIG. 6. Comparison between the  $g$  shifts of  $Gd^{3+}$  ions in TmP and the magnetic susceptibility of TmP.  $1/X$  is in arbitrary units.

this section we would like to review some existing theories on the  $g$  value and the linewidth.

#### A. $g$ -shift due to Gd-host exchange

We consider the situation in which the exchange interaction between a  $Gd^{3+}$  ion and the surrounding rare-earth ions is isotropic. The Hamiltonian of  $Gd^{3+}$  is written

$$\mathcal{H} = g_{Gd} \mu_B \vec{S}_{Gd} \cdot \vec{H} + \sum_j J_j \vec{S}_{Gd} \cdot \vec{S}_{RE}^j, \quad (1)$$

where the first and second terms represent the Zeeman and exchange energies, respectively.  $g_{Gd}$  is the  $g$  value of the isolated  $Gd^{3+}$  ion;  $\mu_B$  is the Bohr magneton;  $S_{Gd}$  and  $S_{RE}^j$  represent the spin of  $Gd^{3+}$  and the host rare-earth ion, respectively; and  $J_j$  is the exchange interaction coefficient of  $Gd^{3+}$  and its  $j$ th host rare-earth neighbor.

Following the theory of Hutchings *et al.*,<sup>5</sup> the  $g$  shift of  $Gd^{3+}$  at zero temperature can be given as

$$\Delta g = \frac{J(0)}{\mu_B H} \langle 0' | S_{RE}^z | 0' \rangle, \quad (2)$$

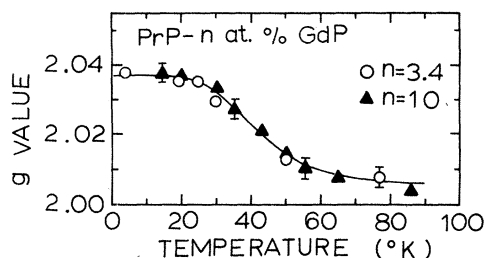


FIG. 7. Temperature dependence of the  $g$  value of  $Gd^{3+}$  in PrP- $n$ -at. % GdP ( $n=3, 4, 10$ ).

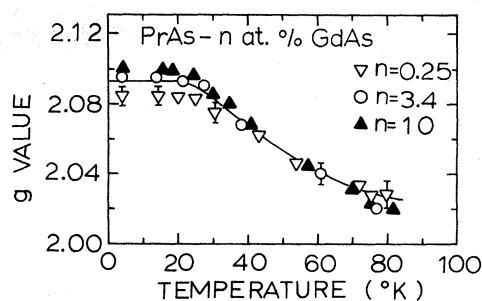


FIG. 8. Temperature dependence of the  $g$  value of  $Gd^{3+}$  in PrAs- $n$ -at. % GdAs ( $n=0.25, 3, 4, 10$ ).

with

$$J(0) \equiv \sum_j J_j, \quad (3)$$

where we have considered that the applied magnetic field is along the  $z$ -axis, and  $|0'\rangle$  represents the perturbed wave function of the ground state of a host rare-earth ion in the magnetic field.

$$|0'\rangle = |0\rangle + \sum_m \frac{\langle m | \mathcal{H}_z | 0 \rangle}{E_0 - E_m} |m\rangle, \quad (4)$$

with

$$\mathcal{H}_z = \mu_B \vec{H} \cdot (\vec{L}_{RE} + 2\vec{S}_{RE}), \quad (5)$$

where  $|0\rangle$  and  $|m\rangle$  represent the crystal-field-only wave functions<sup>6</sup> of the host ground state and the host excited state, respectively. Equation (2) can be interpreted as meaning that the  $g$  shift of  $Gd^{3+}$  is proportional to the isothermal susceptibility of the host rare-earth ion; and the exchange interaction coefficient  $J(0)$  can be obtained if we measure the  $g$  shift of  $Gd^{3+}$  at zero temperature and if the wave functions and the crystal-field splittings of the host rare-earth ions are known. As long as the exchange energy  $J(0) S_{Gd} S_{RE}$  ( $S_{Gd} = \frac{7}{2}$ ; for  $Pr^{3+}$  and  $Tm^{3+}$ ,  $S_{RE} = 1$ ) is small compared to the crystal-field splittings, where in practice the only important comparison is to the crystal-field splitting from the ground to the first excited

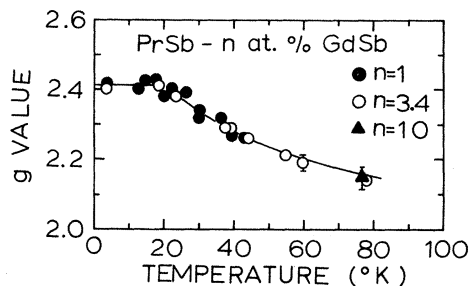


FIG. 9. Temperature dependence of the  $g$  value of  $Gd^{3+}$  in PrSb- $n$ -at. % GdSb ( $n=1, 3, 4, 10$ ).

state, this theoretical prediction, that the  $g$  shift of  $Gd^{3+}$  is proportional to the isothermal susceptibility of the host-rare-earth ion, holds at any temperature. The generalization of Eq. (2) to all temperatures is

$$\Delta g = \frac{\lambda-1}{\lambda} \frac{J(0)}{\mu_B^2} \chi_{CF}, \quad (6)$$

where  $\lambda$  and  $\chi_{CF}$  are the Landé factor of the host and the crystal-field-only susceptibility of the host, respectively.

The isothermal crystal-field-only susceptibility has been calculated<sup>7</sup> for  $Tm^{3+}$  and  $Pr^{3+}$  in the NaCl structure, and there are a number of measurements<sup>8,9</sup> of the isothermal susceptibility of the thulium and praseodymium monopnictides. Both the theoretical and experimental isothermal susceptibilities are of the Van Vleck type and are almost temperature independent below liquid-He temperature. This indicates that one may obtain  $J(0)$  by measuring the  $g$  shift of  $Gd^{3+}$  at liquid-He temperature. (In fact, as discussed below, we have measured the  $g$  shift over a substantial range of temperature, and the value of  $J(0)$  giving the scaling between  $\Delta g$  and  $\chi$  at the lowest temperatures also gives excellent agreement for increasing temperature.)

When there are exchange interactions between the host rare-earth ions, Eq. (6) becomes

$$\Delta g = \frac{\lambda-1}{\lambda} \frac{J(0)}{\mu_B^2} \chi_{CF} / \left[ 1 - 2J'(0) \left( \frac{\lambda-1}{\lambda} \right)^2 \frac{\chi_{CF}}{\mu_B^2} \right], \quad (7)$$

where  $J'(0)$  is the total exchange interaction coefficient between the host rare-earth ions.

### B. Theory of the linewidth

The theory of the temperature dependence of the linewidth for a magnetic impurity in a magnetic host has been investigated by Moriya and Obata.<sup>10</sup> Their theory predicts that the EPR linewidth of the magnetic impurity is proportional to the auto-correlation function of the spin fluctuations of the

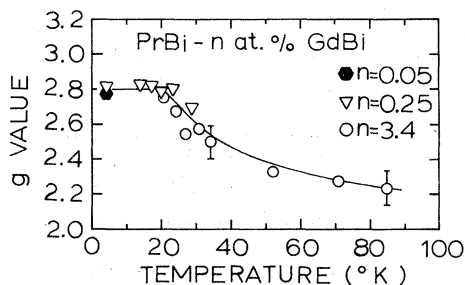


FIG. 10. Temperature dependence of the  $g$  value of  $Gd^{3+}$  in  $PrBi-n$ -at. %  $GdBi$  ( $n=0.05, 0.25, 3.4$ ).

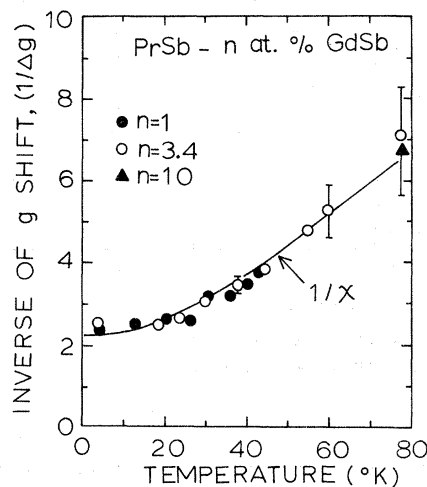


FIG. 11. Comparison between the  $g$  shifts of  $Gd^{3+}$  ions in  $PrSb$  and the magnetic susceptibility of  $PrSb$ .  $1/\chi$  is in arbitrary units.

host magnetic ion. They concluded that the auto-correlation function is approximately given by  $kT$  times the difference between the isothermal and isolated susceptibilities of the host material,

$$\Delta H = AkT(\chi_T - \chi_{iso}). \quad (8)$$

Here  $A$  is a constant, and  $\chi_T$  and  $\chi_{iso}$  are the isothermal and isolated susceptibilities of the host magnetic ion, respectively. The physical significance of Eq. (8) is that the population fluctuation in the excited states of the  $Pr^{3+}$  and  $Tm^{3+}$  ions contributes to the line broadening of the  $Gd^{3+}$  impurity. This means that we expect the linewidth of  $Gd^{3+}$  to increase sharply as the temperature is raised to the order of the crystal-field splitting to the first excited state of the host rare-earth ions; and if the temperature is high compared to the

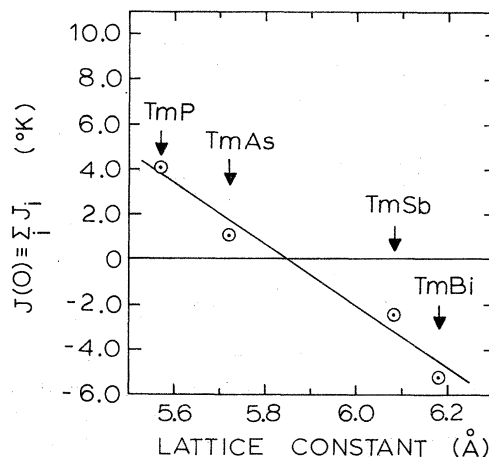


FIG. 12. Exchange interaction between  $Gd^{3+}$  and  $Tm^{3+}$  in  $TmX$ . The horizontal axis is lattice constant.

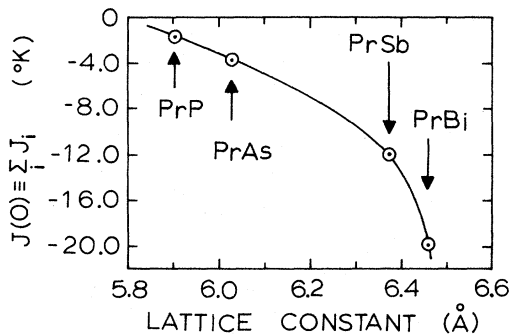


FIG. 13. Exchange interaction between  $Gd^{3+}$  and  $Pr^{3+}$  in  $PrX$ . The horizontal axis is lattice constant.

overall crystal-field splitting, we expect the linewidth to be temperature independent. As discussed in the next section, the isothermal and isolated susceptibilities are directly related to the crystal-field splittings. This means that the measurements of the EPR linewidth of  $Gd^{3+}$  can give very useful information about the crystal-field splittings of the host rare-earth ion.

#### IV. EXPERIMENTAL RESULTS AND DISCUSSION

The observed EPR line shapes are Dysonian. However, as can be seen from Fig. 2, the shapes are not markedly different from true Lorentzian. In this case, the resonant field can be found using the analysis method of Peter *et al.*<sup>11</sup> Occasionally, when the linewidths are relatively wide, we have used a modification<sup>12</sup> of the technique of Peter *et al.* to obtain the resonant fields.

The temperature dependence of the experimentally observed  $g$  values for  $Gd$  diluted in  $TmX$  ( $X=P, As, Sb$ ) are shown in Figs. 3–5. The  $g$  shifts with respect to the high temperature behavior are positive for  $TmP$  and  $TmAs$  hosts, and

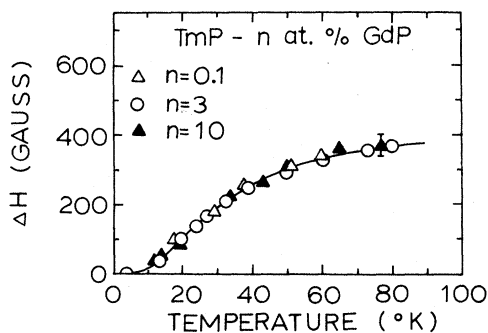


FIG. 14. Temperature dependence of the EPR linewidths of  $Gd^{3+}$  in  $TmP-n$ -at.%  $GdP$  ( $n=0.1, 3, 10$ ). The solid curve represents a fit of the data to the equation  $\Delta H = 970 (0.25 e^{-30/T} + 3.6 e^{-66/T} + 0.36 e^{-240/T})/Z$  G, where  $Z = 1 + 3 e^{-30/T} + 3 e^{-66/T} + e^{-193/T} + 3 e^{-234/T} + 2 e^{-240/T}$ .

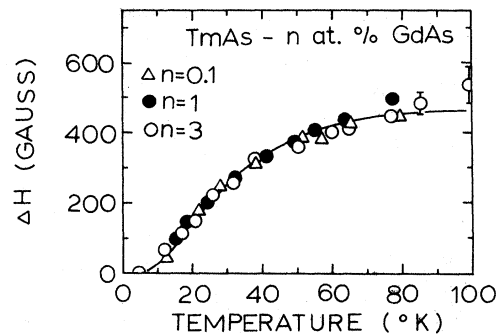


FIG. 15. Temperature dependence of the EPR linewidths of  $Gd^{3+}$  in  $TmAs-n$ -at.% ( $n=0.1, 1, 3$ ). The solid curve represents a fit of the data to the equation  $\Delta H = 1178 (0.25 e^{-28/T} + 3.6 e^{-61.6/T} + 0.36 e^{-218/T})/Z$  G, where  $Z = 1 + 3 e^{-28/T} + 3 e^{-61.6/T} + e^{-180/T} + 3 e^{-218/T} + 2 e^{-225/T}$ .

are negative for  $TmSb$  as host. As discussed below, this indicates a change in sign of the  $Gd^{3+}$ - $Tm^{3+}$  exchange interaction on going from phosphide and arsenide to the antimonide and bismuthide.

At low temperatures the variation of the  $g$  values with temperature flattens out as expected for the Van Vleck type host susceptibility. The  $g$  shifts  $\Delta g$  are found by subtracting the value for the isolated  $Gd^{3+}$  ion, 1.991, from the experimentally observed  $g$  values. As shown in Fig. 6, as predicted by the theory given in Sec. III A, for  $Gd^{3+}$  in  $TmP$  the temperature dependence of  $1/\Delta g$  is in close agreement with that of  $1/\chi$ , the inverse of the isothermal susceptibility. Similar behavior is found<sup>12</sup> for  $Gd^{3+}$  in  $TmAs$  and  $TmSb$ . In addition, we have also observed the  $Gd^{3+}$  resonance in  $TmBi$  at 4.2 °K with the  $g$  value equal to  $1.04 \pm 0.02$ .

The  $g$ -value variation with temperature in the  $PrX$  compounds is shown in Figs. 7–10. The  $g$  shifts are large for  $PrSb$  and  $PrBi$ , while they are

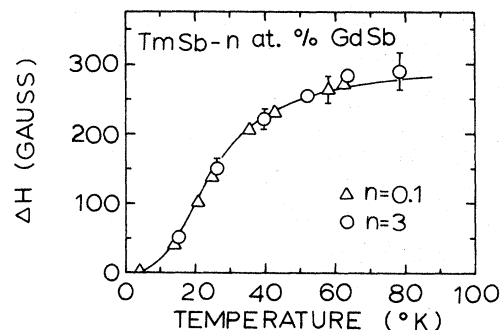


FIG. 16. Temperature dependence of the EPR linewidths of  $Gd^{3+}$  in  $TmSb-n$ -at.%  $GdSb$  ( $n=0.1, 3$ ). The solid curve represents a fit of the data to the equation  $\Delta H = 743 (0.25 e^{-25/T} + 3.6 e^{-55/T} + 0.36 e^{-195/T})/Z$  G, where  $Z = 1 + 3 e^{-25/T} + 3 e^{-55/T} + e^{-160/T} + 3 e^{-195/T} + 2 e^{-201/T}$ .

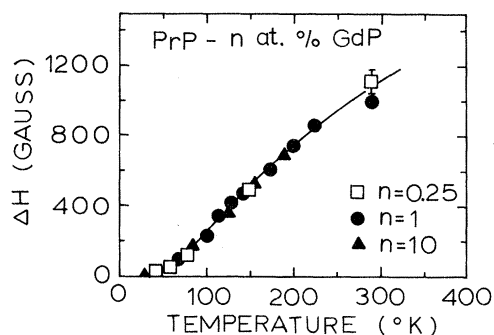


FIG. 17. Temperature dependence of the EPR linewidths of  $Gd^{3+}$  in  $PrP-n$ -at.%  $GdP$  ( $n=0.25, 1, 10$ ). The solid curve represents a fit of the data to the equation  $\Delta H = 2797 (0.25 e^{-128/T} + 6.25 e^{-400/T})/Z$  G, where  $Z = 1 + 3 e^{-128/T} + 2 e^{-224/T} + 3 e^{-400/T}$ .

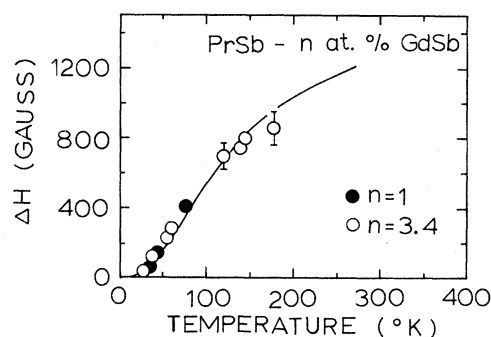


FIG. 19. Temperature dependence of the EPR linewidths of  $Gd^{3+}$  in  $PrSb-n$ -at.%  $GdSb$  ( $n=1, 3.4$ ). The solid curve represents a fit of the data to the equation  $\Delta H = 2520 (0.25 e^{-73/T} + 6.25 e^{-239/T})/Z$  G, where  $Z = 1 + 3 e^{-73/T} + 2 e^{-127/T} + 3 e^{-239/T}$ .

small for  $PrP$ . As shown in Fig. 11, just as for the  $TmX$  hosts, the temperature dependence of  $1/\Delta g$  is in good agreement with that of  $1/\chi$  for  $PrSb$  as host. Just as for the  $TmX$ -host results,  $\Delta g$  here is the difference between the experimental  $g$  value and 1.991. Similar behavior<sup>12</sup> is found for  $PrP$ ,  $PrAs$ , and  $PrBi$  as hosts.

The total exchange interaction  $J(0)$  between a  $Gd^{3+}$  ion and the surrounding host rare-earth ions can be obtained from the value of the  $g$  shift at liquid-He temperature. This information is obtained from Eq. (7) by using the measured  $g$  shifts and susceptibilities.<sup>8,9,13(a)</sup> Figures 12 and 13 show the relationship between  $J(0)$  and the host lattice constant. For  $PrX$ ,  $J(0)$  increases in magnitude (becomes more negative) with increasing lattice parameter, while for  $TmX$ ,  $J(0)$  changes sign from positive to negative with increasing lattice parameter.

The exchange-induced  $g$  shifts are quite large and recall those observed<sup>13(b), 13(c)</sup> for  $Eu^{2+}$ ,  $Gd^{3+}$ ,

and  $Mn^{2+}$  in the singlet-ground-state semiconductors  $SmS$ ,  $SmSe$ , and  $SmTe$ . The functional dependence of the observed exchange on lattice parameter is quite different from the semiconductor case,<sup>13(c)</sup> however. This difference could be related to the metallic nature of the monopnictides studied in the present work.

The temperature dependence of the experimentally observed EPR linewidths of  $Gd^{3+}$  in  $TmP$ ,  $TmAs$ ,  $TmSb$ ,  $PrP$ ,  $PrAs$ ,  $PrSb$ , and  $PrBi$  are shown in Figs. 14–20, respectively. (The linewidths are plotted after subtracting the residual linewidth,  $\Delta H$  at  $T=0$ °K, from the observed linewidths.) Qualitatively, the most striking feature of these results is the sharply increasing linewidth with increasing temperature (exponentially increasing at temperatures lower than the energy splitting to the first crystal-field excited state of the host rare-earth ion).

The theoretical linewidth is given by Eq. (8). Using the nomenclature of Ref. 7 (see Eqs. 39–41

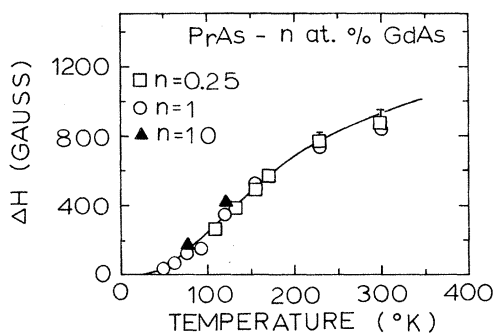


FIG. 18. Temperature dependence of the EPR linewidths of  $Gd^{3+}$  in  $PrAs-n$ -at.%  $GdAs$  ( $n=0.25, 1, 10$ ). The solid curve represents a fit of the data to the equation  $\Delta H = 2250 (0.25 e^{-115/T} + 6.25 e^{-360/T})/Z$  G, where  $Z = 1 + 3 e^{-115/T} + 2 e^{-203/T} + 3 e^{-360/T}$ .

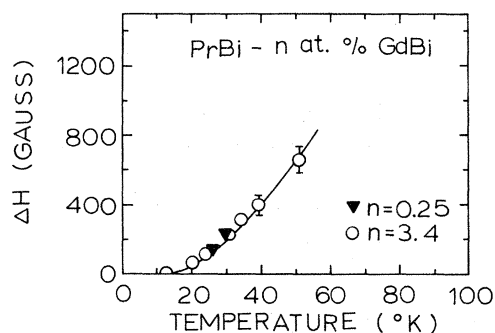


FIG. 20. Temperature dependence of the EPR linewidths of  $Gd^{3+}$  in  $PrBi-n$ -at.%  $GdBi$  ( $n=0.25, 3.4$ ). The solid curve represents of the data to the equation  $\Delta H = 7600 (0.25 e^{-67/T} + 6.25 e^{-203/T})/Z$  G, where  $Z = 1 + 3 e^{-67/T} + 2 e^{-116/T} + 3 e^{-203/T}$ .

TABLE I. Experimentally observed  $E(\Gamma_4) - E(\Gamma_1)$  crystal-field splitting of  $Tm^{3+}$  in  $TmX$  and  $Pr^{3+}$  in  $PrX$  ( $X=P, As, Sb, Bi$ ) intermetallic compounds.

	$Tm^{3+}$		$Pr^{3+}$		
	$E(\Gamma_4) - E(\Gamma_1)$ (°K)		$E(\Gamma_4) - E(\Gamma_1)$ (°K)		
	Present experiment (linewidth analysis)	Neutron scattering <sup>a</sup>	Present experiment (linewidth analysis)	Neutron scattering <sup>b</sup>	
TmP	30 ± 3	≈ 32	PrP	128 ± 15	127 ± 12
TmAs	28 ± 3	≈ 31	PrAs	115 ± 15	117 ± 8
TmSb	25 ± 3	≈ 25	PrSb	73 ± 10	73 ± 4
			PrBi	67 ± 10	67 ± 4

<sup>a</sup>Reference 14.<sup>b</sup>Reference 15.

of Ref. 7), the difference  $\chi_T - \chi_{iso}$  is equal to  $\chi_R$ , the repopulation contribution<sup>7</sup> to the susceptibility. Therefore we take the linewidth as being proportional to  $\chi_R$ . For the crystal-field parameter<sup>6</sup>  $x$ , giving the ratio of fourth to sixth-order anisotropy close to  $-1$ , as is indicated experimentally for the rare-earth mononictides, this gives

$$\Delta H = a(0.25e^{-E(\Gamma_4)/kT} + 3.6e^{-E(\Gamma_5^{(2)})/kT} + 0.36e^{-E(\Gamma_5^{(1)})/kT})/Z \text{ (for } Tm^{3+}) \quad (9)$$

$$\Delta H = b(0.25e^{-E(\Gamma_4)/kT} + 6.25e^{-E(\Gamma_5)/kT})/Z \text{ (for } Pr^{3+}), \quad (10)$$

where  $a$  and  $b$  are some numerical coefficients, and  $Z$  is the single-ion partition function.

Generally, accurate calculations of  $a$  and  $b$  are very complicated. However, we are interested in the determination of  $E(\Gamma_4)$  [since determining  $E(\Gamma_4)$  fixes all the crystal-field splittings for specified  $x$ ] and not in the scaling factors  $a$  and  $b$ . Let us consider Fig. 14 [TmP- $n$ -at. % GdP] as an example. The experimental data fit, for TmP- $n$ -at. % GdP,

$$\Delta H = 970(0.25e^{-30/T} + 3.6e^{-66/T} + 0.36e^{-240/T})/Z \text{ G} . \quad (11)$$

Here the value of the scaling factor, 970, was chosen by adjusting the scaling factor  $a$  in Eq. (9) until the theoretical curve fits the experimental data at all temperatures. This result indicates that the  $\Gamma_4$  and  $\Gamma_5^{(2)}$  states are at 30 and 66 °K above the  $\Gamma_1$  ground state, respectively. These values are consistent with our values<sup>3(a)</sup> obtained by performing the EPR in the excited  $\Gamma_5^{(2)}$  state of  $Tm^{3+}$  in TmP.

Similar analyses of the linewidth behavior have been performed for all samples, and the results for the crystal-field splittings of  $Tm^{3+}$  are tabulated in Table I. The present results agree

quite well with those obtained from neutron scattering.<sup>14,15</sup>

In all the experiments described above, Gd was used as the probe impurity. We also considered the possibility of using Dy or Er as the probe impurity, but for reasons we will briefly describe, rejected this. To investigate that possibility, we prepared several samples of the type  $n$  at. % DyX in YX,  $n$  at. % DyX in LaX, and  $n$  at. % GdX in YX, where the host is nonmagnetic and  $n$  is less than 10. EPR experiments were done in the temperature range between 4.2 and 150 °K for Dy, and between 4.2 and 300 °K for Gd. (Our experimental results show that the ground state of  $Dy^{3+}$  in LaX and YX is  $\Gamma_6$ , consistent with the experimental results of Davidov *et al.*<sup>16</sup>) We found that the experimentally observed peak-to-peak linewidth of  $Dy^{3+}$  increases sharply ( $\partial\Delta H_{pp}/\partial T \approx 5$  G/°K, and 8 G/°K for  $Dy^{3+}$ : YX, and  $Dy^{3+}$ : LaX, respectively) above 20 °K, and the increase is almost linear in  $T$ . Because of this line broadening,  $Dy^{3+}$  is not suitable as a probe. On the other hand, the linewidth for the EPR of  $Gd^{3+}$  diluted in YX shows little variation with temperature.<sup>12</sup> The temperature-dependent contribution to the linewidth, presumably due to Korringa-type relaxation via the conduction electrons, is 10% or less of that for  $Dy^{3+}$ . This small Korringa-type linewidth for the EPR of  $Gd^{3+}$  in the YX compounds shows that  $Gd^{3+}$  is an appropriate choice of magnetic impurity probe for the EPR experiments of interest in the paramagnetic hosts. In fact, the lack of  $Gd^{3+}$  concentration dependence of the linewidths shown in Figs. 14–20 indicates that the Korringa-type contribution to the temperature-dependent line width is even smaller for  $Gd^{3+}$  in TmX and PrX.

Our discussion in this paper has been confined to the case where the host material is paramagnetic. However, our experimental method can be applied to antiferromagnetic host materials such as

Tb<sub>2</sub>Y<sub>1-x</sub>X (x ≥ 0.4) and CeX. Our preliminary results<sup>17</sup> for TbP-5-at. % GdP indicate that the Gd<sup>3+</sup> *g* shifts are strongly affected by the staggered susceptibility. We did not see any line broadening of Gd<sup>3+</sup> near the Néel temperature.

## ACKNOWLEDGMENTS

We would like to thank Dr. W. L. Gordon for many discussions. We thank Dr. W. M. Walsh for sending us a preprint copy of Ref. 3b.

\*This paper is based on results reported in the Ph.D. thesis of K. Sugawara, Case Western Reserve University.

†Supported in part by NSF Grant No. DMR 74-08033.

<sup>1</sup>B. R. Cooper and O. Vogt, *J. Phys. (Paris)* **32**, C1-958 (1971).

<sup>2</sup>W. J. L. Buyers, in the Proceedings of the 20th Annual Conference on Magnetism and Magnetic Materials, San Francisco, 1974 (to be published).

<sup>3</sup>(a) K. Sugawara, C. Y. Huang, and B. R. Cooper, in the Proceedings of the 20th Annual Conference on Magnetism and Magnetic Materials, San Francisco, 1974 (to be published). (b) After completion of the present work, we became aware of the work by C. Rettori, D. Davidov, A. Grayevsky, and W. M. Walsh [preceding paper, *Phys. Rev. B* **11**, 4450 (1975)]. This work examines the *g*-shifts for Gd substituted into TmSb, TmBi, PrSb, PrBi, and PrTe, and uses these results to deduce the Gd-Tm or Gd-Pr exchange coupling.

<sup>4</sup>E. D. Jones, *Phys. Rev.* **180**, 455 (1969).

<sup>5</sup>M. T. Hutchings, C. G. Windsor, and W. P. Wolf, *Phys. Rev.* **148**, 444 (1966).

<sup>6</sup>K. R. Lea, M. J. M. Leask, and W. P. Wolf, *J. Phys. Chem. Solids* **23**, 1381 (1962).

<sup>7</sup>B. R. Cooper, R. C. Fedder, and D. P. Schumacher, *Phys. Rev. Lett.* **18**, 744 (1967); B. R. Cooper, R. C. Fedder, and D. P. Schumacher, *Phys. Rev.* **163**, 506 (1967); **168**, 654 (E) (1968).

<sup>8</sup>G. Busch, A. Menth, O. Vogt, and F. Hulliger, *Phys. Lett.* **19**, 622 (1966); G. Busch, O. Vogt, O. Marinček, and A. Menth, *Phys. Lett.* **14**, 262 (1965).

<sup>9</sup>E. Bucher, K. Andres, J. P. Maita, A. S. Cooper, and L. D. Longinotti, *J. Phys. (Paris) C* **1**, 115 (1970).

<sup>10</sup>T. Moriya and Y. Obata, *J. Phys. Soc. Jpn.* **13**, 1333

(1958).

<sup>11</sup>M. Peter, D. Shaltiel, J. H. Wernick, H. J. Williams, J. B. Mock, and R. C. Sherwood, *Phys. Rev.* **126**, 1395 (1962).

<sup>12</sup>K. Sugawara, Ph.D. thesis (Case Western Reserve University, 1974) (unpublished).

<sup>13</sup>(a) T. Tsuchida and W. E. Wallace, *J. Appl. Phys.* **43**, 2885 (1965); (b) F. Mehran, K. W. H. Stevens, R. S. Title, and F. Holzberg, *Phys. Rev. Lett.* **27**, 1368 (1971); (c) R. J. Birgeneau, E. Bucher, L. W. Rupp, Jr., and W. M. Walsh, Jr., *Phys. Rev. B* **5**, 3412 (1972).

<sup>14</sup>For TmSb we used the value for  $E(\Gamma_4) - E(\Gamma_1)$  from R. T. Birgeneau, E. Bucher, L. Passell, and K. C. Turberfield, *Phys. Rev. B* **4**, 718 (1971). As shown in Table I, this value is in very close agreement with that we found from analysis of the EPR linewidth. For TmP and TmAs we used the value for  $E(\Gamma_4) - E(\Gamma_1)$  found from analysis of the EPR linewidth. As shown in Table I, this value is in good agreement with the values subsequently reported found by neutron scattering [R. J. Birgeneau, E. Bucher, J. P. Maita, L. Passell, and K. C. Turberfield, *Phys. Rev. B* **8**, 5345 (1973); H. L. Davis and H. A. Mook, *AIP Conf. Proc.* **18**, 1068 (1974)].

<sup>15</sup>K. C. Turberfield, L. Passell, R. J. Birgeneau, and E. Bucher, *Phys. Rev. Lett.* **25**, 752 (1970); *J. Appl. Phys.* **42**, 1746 (1971).

<sup>16</sup>D. Davidov, E. Bucher, L. W. Rupp, Jr., L. D. Longinotti, and C. Rettori, *Phys. Rev. B* **9**, 2879 (1974).

<sup>17</sup>C. Y. Huang, K. Sugawara, and B. R. Cooper, in Proceedings of the 20th Annual Conference on Magnetism and Magnetic Materials, San Francisco, 1974 (to be published).